Bolt Looseness Detection in Brake Disc of High-Speed Rail Using Wavelet Packet Decomposition and 1D Convolutional Neural Network

Huifang Xiao, Zedong Li, Xuyang Guan and Zhaoxin Liu

School of Mechanical Engineering, University of Science and Technology Beijing, Beijing 100083, PR China.
E-mail: huifangxiao@ustb.edu.cn

(Received 4 August 2023; accepted 3 December 2023)

The effective and in-time detection of bolt looseness in the brake disc of high-speed rail is of great significance to ensure the safe operation of the train. The hammer tapping method is one of the most widely used methods for bolt looseness detection. Due to the complex structure of the brake disc, the vibration characteristics associated with bolt looseness are coupled with the transmission path from the head of the bolt through the brake disc to the sensors, which make it difficult to quantitively identify the bolt looseness. In this work, a method based on wavelet packet decomposition and a one-dimensional convolutional neural network (1D CNN) is proposed to quantitively detect the bolt looseness of brake disc. Firstly, the vibration signals collected from the two sensors mounted on the nut side are fused by autocorrelation summation to reduce the influence of transmission path. Secondly, the fused signal is decomposed to sub signals in low frequency and high frequency components by wavelet packet decomposition. The relative difference of wavelet packet energy among sub signals is extracted as the features to enhance the difference among different degrees of looseness. Finally, the 1D CNN model is established and trained by the features of energy relative difference to quantitively identify the bolt looseness. To validate the effectiveness of the proposed method, an experimental platform for bolt looseness detection in brake disc is constructed. Compared with the single-channel 1D CNN and fused signal-1D CNN models, the accuracy of the proposed method is approximately 97%, which confirms the superiority of the proposed method.

1. INTRODUCTION

The different components of a brake disc in high-speed rail are connected and mounted together through bolts. During the long-term operation, bolts are prone to looseness due to the variable speeds and loads in the periodic speeding-braking working conditions as well as the dramatic variation of temperature.[1,2] When bolt looseness occurs, the brake disc may run out of the effective braking load and be unable to stop the high-speed train within the effective brake distance, which may cause severe accidents. Therefore, it is of great importance to effectively detect the bolt looseness for the safe operation of high-speed rail.

In recent years, different detection methods for bolt looseness in different industrial applications are developed. The hammer tapping method is one of the most widely used methods for bolt looseness detection in flange connection and steel pillar connection.[3,4] A hammer is used to tap the head of the bolt to generate an excitation signal. Different types of response signals at different locations of the bolts or the connected components can be acquired using different transducers, including the acoustic signal through acoustic sensors,[5–9] the stress wave signal through piezoelectric transducer[10–14] and vibration signal through accelerometers.[15–17] The hammer tapping[5–9,14] or exciter[10–13,17] are usually used to excite the flat plate bolted connections to produce acoustic signals and stress wave signals. Then, the signal processing methods, such as empirical mode decomposition (EMD),[8] variational mode decomposition (VMD),[15] and wavelet package decomposition (WPD)[13,17] are often combined with energy entropy[6,13,17] and multi-scale entropy[14] damage indicators for quantitative analysis. The machine learning methods, such as, back-propagation neural network (BP NN),[8] gradient boosting decision tree (GBDT),[9] and support vector machine (SVM),[7,14,15] are introduced to identify the different degree of bolts looseness. For the non-tapping method, the image methods that use vision cameras to capture bolt loosening images are also widely used in the structural steel connections of high bridges and cable towers. The captured images are usually combined with the deep learning method to identify bolt looseness taking the advantage of deep learning adaptive feature extraction and high recognition accuracy in image recognition.[19–21] In summary, the piezoelectric sensors are susceptible to temperature and the collected signals lose some high-frequency information, which are not suitable for complex structures of the brake disc. For bolt looseness monitoring based on acoustic signal and image signal, the data collection is susceptible to the influence of external environment and not easy to obtain. The bolt looseness detection methods based on signal processing is dependent on a great deal of professional knowledge and experience, and the qualitative analysis is prone to omissions and misjudgments.

The monitoring methods based on vibration signal can effectively reflect the time-frequency characteristics of the complex structure of the brake disc. The acceleration sensors have the advantage of small size, high sensitivity, and convenience, which are easily arranged on the brake disk. For example, Sun et al.[15] proposed a method by combining the variational modal decomposition and singular value decomposition to process the vibration signal of bolt looseness. The permutation entropy of decomposed signals is extracted as the input feature to the support vector machine to detect the bolt loosening detection. Champati et al.[16] used the impact hammer technique to obtain the acceleration response of bolted steel structures. The frequency response data obtained by input response and output response are used to extract the modal strain energy to identify the bolt damage. Zhang et al.[17] proposed a quantitative index based on the wavelet packet energy entropy to identify the different degree of bolt looseness. The vibration responses of bolts under different states obtained from tightening and loosening are used to verify the effectiveness of index. Therefore, the vibration signal can be taken as the response for the looseness states of bolt connections.

In these previous studies, the structures for bolt looseness detection are mostly two flat plates connected by the bolts, as shown in Fig. 1(a). The hammer tapping method is applied by tapping and measuring on the same side of the bolt and the obtained signals are single-shock waves attenuated in a short period. The responses collected on the plates are weakly coupled due to the simple structure of two flat plates. However, the structure of the brake disc in high-speed rail is much more complicated, which comprised of two discs with gap structure and these components are generally circumferential connected using twelve high-strength bolts, as shown in Fig. 1(b). Due to the complex structure of the brake disc, the signal will transmit to the nut side through different components of the brake disc when the head of bolt is tapped by a force hammer. The vibration characteristics associated with bolt looseness are coupled with the transmission path. It is difficult to quantitively identify the bolt looseness with a single sensor and the feature indicator methods for the brake disc. Therefore, the effect of transmission path on the collected vibration signals should be eliminated for the quantitively bolt looseness detection. In addition, the vibration signals associated with bolt looseness is nonlinearity and non-stationarity and is composed of wide-range frequency components, which are resulted from the coupling interaction between different components of the brake disc with complex structure. The wavelet packet decomposition has the advantages of obtaining sub-signals with low and high frequency at multiple levels by decomposing the frequency band, which is applicable to the coupled signal of bolt looseness. The one-dimensional convolutional neural network (1D CNN) has the advantages of selecting the effective feature for classification adaptively, which avoids the shortcomings of feature omission through manual selection and improves the classification accuracy.

In this work, a method based on wavelet packet decomposition and a one-dimensional convolutional neural network (WPD-1D CNN) is proposed to detect the bolt looseness of brake disc. To eliminate the effect of transmission path on the vibration signals, two sensors are mounted on the nut side to collect the vibration responses with the excitation generated by tapping the bolt head on the other side of the disc. The vibration signals collected from the two sensors are further fused by autocorrelation summation to reduce the influence of transmission path from head of bolt through the brake disc to the sensor positions. Then, the fused signal is decomposed by wavelet packet decomposition to sub signals of low frequency and high frequency components. The relative differences of the wavelet packet energy of sub signals are extracted as the features of bolt looseness to enhance the difference among different degrees of looseness. Finally, the 1D CNN model is constructed. The samples based on relative energy difference of bolt under different torques are used to train the 1D CNN model to quantitively identify the bolt looseness.

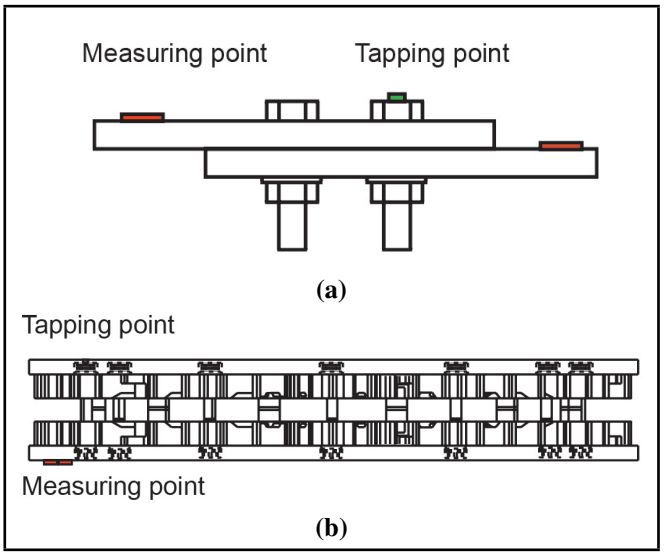

Figure 1. Structure of the bolt connection for (a) simple two flat plates and (b) brake disc.

The paper is organized as follows. The detailed steps for detecting the bolt looseness of the brake disc by the proposed method are introduced in Section 2, including signal autocorrelation summation, wavelet packet decomposition, relative difference of wavelet packet energy, and 1D CNN model. In Section 3, a test rig of bolt looseness of brake disc is established, and the proposed method is applied and validated to bolt looseness identification. The paper is concluded in Section 4.

2. METHODOLOGY

2.1. Structure of Brake Disc in High-speed Rail

High speed railway brake discs mainly consist of discs with gap structure, wheels, and bolts. The brake disc is mounted and connected using the twelve high-strength bolts. Bolts are susceptible to looseness during long-term operation due to the varying speeds and loads in periodic working conditions, as well as the significant temperature fluctuations. To detect the bolt looseness, as shown in Fig. 2(a), from the front side of the brake disc, the head of the bolt is impacted by an impact hammer to apply excitation. At the back side of the brake disc,

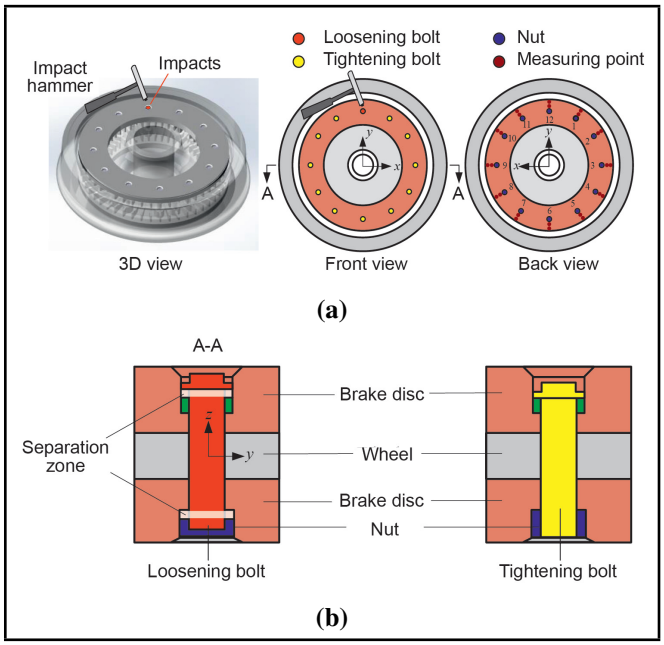

Figure 2. Structure of wheel-type brake disc and bolt (a) Bolt position and measuring point arrangement (b) Sketch of the brake disc bolt joint interface.

the two measurement points are arranged near the nut to collect signals. When the bolt is loosened, as shown in Fig. 2(b), the interface between head of bolt and brake disc is not fully contact, which generates a separation zone, and the interface between nut and brake disc also presents the separation zone. This separation zone causes energy loss in signal transmission as well as complexity in the transmission path from head of bolt through the brake disc to sensors. However, when the bolt is tightened, there is no separation zone in the contact interface of head of bolt and brake discand the interface of nut and brake disc. Therefore, different vibration responses will be generated when the excitation passes through bolts with different degrees of looseness.

2.2. Proposed Method

According to the characteristics of the bolt connection of the brake disc in a high-speed rail, a bolt loosening detection method base on WPD-1D CNN is proposed. The flow block diagram of the proposed method is shown in Fig. 3. The detailed steps are as listed below.

Step 1: Excitation is generated by tapping the head of the bolt with a force hammer. The acceleration sensors are arranged at two points near the bolt nut and used to collect the vibration signals. To simulate the different degrees of bolt looseness, torque wrenches are used to control the bolt looseness.

Step 2: The signals collected from the sensors at the two positions are fused by autocorrelation summation and the fused signals are normalized.

Step 3: The fused signals of the bolt are decomposed to obtain the frequency sub signals by wavelet packet decomposition (WPD). Then, the energy values of sub signals are calculated. The relative difference of energy for sub signals are selected as the feature indicator to divide the loosening and tightening state of the bolt.

Step 4: The 1D CNN model is established to quantitively detect the bolt looseness. The input samples are constructed based on energy relative difference, which are divided into training test and testing set. The training datasets are used to train the 1D CNN and the testing datasets are used to validate the effectiveness of the model. The validated model can be further used to quantitatively identify the looseness state of brake disc bolts.

2.2.1. Autocorrelation summation

The autocorrelation function describes the degree of correlation between the values of the signals at any two different times, linking the cross-spectrum of the signals between the two sensor points to their respective auto-spectra.[22,23] It can be used to determine how much of the output signal comes from the input signal and can correct the error caused by the noise source being connected to the measurement. The characteristics of the vibration signal after noise reduction are not obvious, so it is not suitable for feature extraction directly. Therefore, autocorrelation is used to process the vibration models collected by the two sensors mounted on the brake disc nut, and the autocorrelation signals are added together. The sum of discretized autocorrelation functions can be expressed as:[24]

$$\psi_1(m) = \sum_{n=-\infty}^{+\infty} f_1(n) f_1(n-m); \tag{1}$$

$$\psi_2(m) = \sum_{n=-\infty}^{+\infty} f_2(n) f_2(n-m); \tag{1a}$$

$$\psi(m) = \psi_1(m) + \psi_2(m); \tag{1b}$$

where m is the delay time, $f_1(n)$ and $f_2(n)$ are the vibration signals of sensor 1 and sensor 2, respectively. $\psi_1(m)$ and $\psi_2(m)$ is the autocorrelation signals of sensor 1 and sensor 2, respectively. $\psi(m)$ is the autocorrelation summation signal.

After processing by autocorrelation summation, the amplitude of fused signals is diffused. To increase the comparability between the loosen and tighten vibration signals, the amplitudes of the signals are normalized between $[-1, 1]$. The conversion formula can be expressed as:

$$P(m) = \frac{2\left(\psi(m) - \psi_{min}\right)}{\psi_{max} - \psi_{min}} - 1; \tag{2}$$

where $P(m)$ is the normalized vibration signal, and ψ_{max}, ψ_{min} represent the maximum and minimum values of time series signal, respectively.

2.2.2. Wavelet packet decomposition

Due to the complex structure of the brake disc, the bolt loosening vibration signal is complex and nonlinear.[25] Wavelet packet decomposition (WPD) has great advantages in dealing with non-stationary signals, which can divide the frequency bands of a signal in detail by the low-pass filter and high-pass filter.[17,26,27] It can decompose both the low-frequency and high-frequency components of the original signal into multiple subsequences. The WPD decomposes the entire signal band by

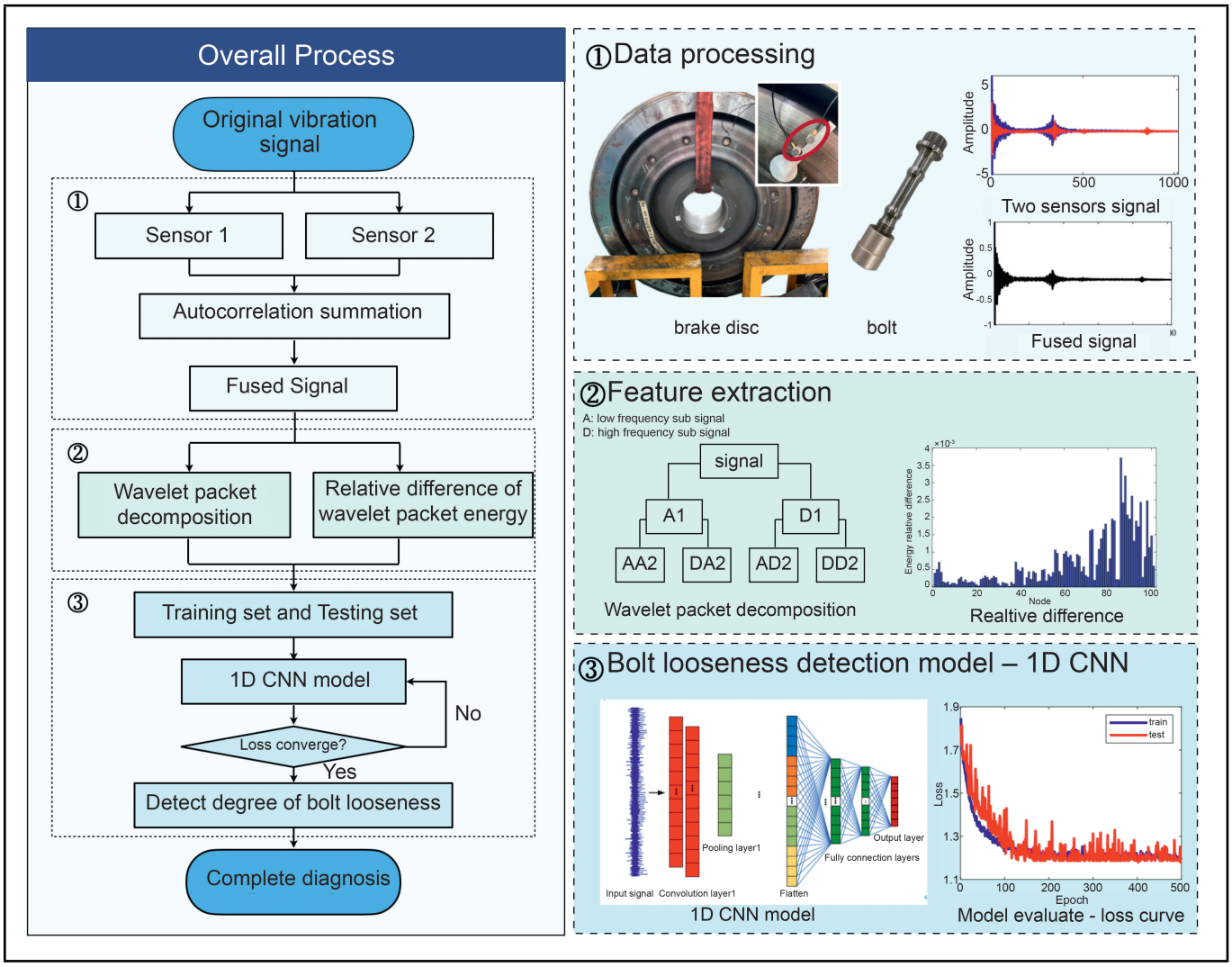

Figure 3. Flowchart of bolt looseness detection.

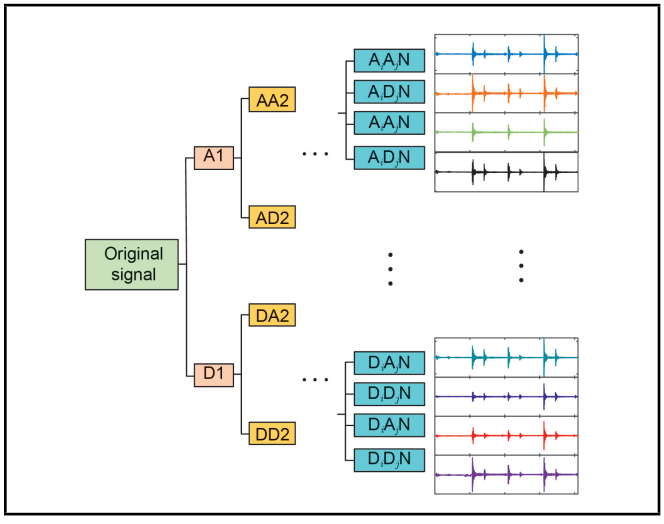

Figure 4. Schematic diagram of the wavelet packet decomposition (WPD).

a tree diagram with one node into two nodes, resulting in several different sub signals, as shown in Fig. 4.

And the wavelet packet decomposition equation is:

$$\begin{cases} P_j^{2i-1}(t) = HP_{j-1}^i(t), & i = 1, 2, \cdots 2^j \\ P_j^{2i}(t) = GP_{j-1}^i(t), & j = 1, 2, \cdots 10 \end{cases}; \tag{3}$$

where H is a low-pass filter and G is a high pass filter, P_j^i is the i-th node obtained by the j-th wavelet packet decomposition.

To effectively remove the noise and retain the useful information in the decomposed sub signals, the energy values in each sub signal are calculated. A higher energy means a larger component of the useful signal in the corresponding frequency band. The energy value corresponding to the ith frequency sub signal is expressed as:[11,17,28]

$$E_i = \sum_{k=1}^{N} \left[p_{j,k}^i\right]^2; \tag{4}$$

where $P_{j,k}^i$ is the the k-th wavelet packet coefficient corresponding to P_j^i and N is the length of the sub signal. The wavelet packet energy vectors are constated as $E = [E_1, E_2, \ldots, E_{2j}]$.

In this work, the fused signal of bolt $P(m)$ is decomposed into 2^{10} sub signals by WPD.[29] If the number of decompositions is small, the differences in the sub-signals are not significant. For the subsequent process of extracting the energy of the sub signals, the number of features is sufficient. The energy features in different frequency sub signals are obtained as the index of the bolt loosening fault. The relative difference between the wavelet packet energy of the loosen sample and

that of the tighten sample is defined to strengthen the feature difference between different degrees of bolt looseness, which is expressed as:[13,28]

$$e_a = \frac{|Er_a - Ef_a|}{Er_a} \times 100\%, \quad a = 1, 2, \cdots 2^N; \tag{5}$$

where e_a is the relative difference between wavelet packet energy of the loosened bolt and tightened bolt, E_{ra} is the root-mean-square value of wavelet packet energy for loosened samples, E_{fa} is the root-mean-square value of wavelet packet energy for tightened samples, and are expressed as:

$$Er_a = \sqrt{\frac{\sum_{k=1}^{K} E_{a,k}^2}{K}}, \quad Ef_a = \sqrt{\frac{\sum_{z=1}^{Z} E_{a,z}^2}{Z}}; \tag{6}$$

where $E_{a,k}$ is the a-th frequency sub signals energy of k-th loose sample, K is the number of loosened samples, $E_{a,z}$ is the a-th frequency sub signals energy of z-th loose sample, Z is the number of tightened samples.

2.2.3. One-dimensional convolutional neural network model

The convolutional Neural Network (CNN) is perhaps the most implemented deep learning algorithm applicable to various applications.[29–31] The vibration signal of bolts is one-dimensional; therefore, a one-dimensional deep convolutional neural network (1D CNN) is established. The 1D CNN mainly consists of an input layer, convolutional layer, pooling layer, flatten layer, fully connected layer, and output layer. The convolutional and pooling layers are stacked several times to extract the hidden feature of input and reduce the dimensionality. The main role of the convolution layer is to compute the convolution operation between the input and convolution kernels. The high-dimensional tensor features are obtained by sliding the convolution kernel over the input. The pooling layer is mainly used to reduce the parameters of the network by down-sampling the high-dimensional feature tensor after the convolution layer. The Max Pooling is used in this work. The flatten layer is used to expand the high-dimensional tensor into a vector to connect the fully connected layers. The output layer is used by SoftMax functions for classification.

For the convolutional layer, the l-th layer output x_c^l is expressed as:

$$x_c^l = f\left(w_c^l * x_{in}^{l-1} + b^l\right); \tag{7}$$

where x_{in}^{l-1} is the input, * is the convolution operation, $f()$ is the nonlinear activate function, w_c^l is the weight of the convolutional layer, and b_c^l is the bias.

The l-th pooling layer is obtained as:

$$x_{down}^p = Maxpooling\left(x_c^l\right); \tag{8}$$

where Maxpooling( ) is the Maximum pooling calculation. The output of the last pooling layer x_{down}^p is flattened as:

$$x_{fl} = flatten(x_{down}^p). \tag{9}$$

The output of the fully connected layer x_{fc} is obtained as:

$$x_{fc} = f\left(x_{fl} * w_{fc} + b_{fc}\right). \tag{10}$$

And the output $\widehat{y}$ of output layer can be obtained as:

$$\widehat{y} = softmax\left(x_{fc}\right). \tag{11}$$

Then, in the back propagation, the weight w and bias b of each layer is updated by minimizing the loss function $J(w, b)$ as:

$$\min J(w, b) = \sum \left(y \log\left(\widehat{y}\right) + (1 - y) \log\left(1 - \widehat{y}\right)\right); \tag{12}$$

where y is true label, $\widehat{y}$ is the predicted label. According to the predicted label, the degree of bolt looseness can be obtained.

To evaluate the performance of the proposed method, the accuracy can be calculated as:[31]

$$accuracy = \frac{TP + FP}{TP + TN + FP + FN}; \tag{13}$$

where TP, FN, TN and FP are the number of true positives, false negatives, true negatives and false positives, respectively. The loss in Eq. (12) and the accuracy in Eq. (13) are used as the evaluation index of 1D CNN model.

3. EXPERIMENTAL TESTS

3.1. Data Acquisition

To verify the effectiveness of the proposed method for detecting bolt looseness, a set of experiments were established. The experimental system is shown in Fig. 5, which included the brake disk with twelve bolts, two accelerators, a D-type impact device, a data acquisition, and a computer. The accelerators were B&K 4394 type, the range of the sampling frequency was 1–25000 Hz. The D-type impact device was produced in Junda Instrument company, the diameter was 20 mm, the length was 75 mm, and the sensitivity was 2.25 mV/N. In the experiment, the sampling frequency was set as 6.4 kHz. The brake disc was assembled using twelve circumferential distributed bolts. The brake disc was suspended in a free state and all the bolts were screwed into fully tighten state. In each experiment, only one bolt was loosened. The torques of the bolt to be tested was adjusted by torque wrench to generate the loosened and tightened working conditions, as listed in Table 1. The torques of 0 N·m, 10 N·m, 20 N·m, 30 N·m, 40 N·m corresponded to the loosen state and the torques of 140 N·m and 160 N·m corresponded to the tighten state. The excitation was applied using a D-type impact device on the head of bolt. The acceleration sensors were mounted at the measuring positions near the nut, as shown in Fig. 2(a), and the measured signals are input to the corresponding channels of the data collector for further analysis.

3.2. Signal Analysis

The time-domain signal and the frequency spectrum of the vibration signals from the sensors are shown in Fig. 6, and the shaded portion in the figure represents the high-frequency region, ranging from 1000–3000 Hz. The time-domain signals had secondary shock peaks for different torques. As shown in 6(i)(a), when the bolt was completely loosened, the peak

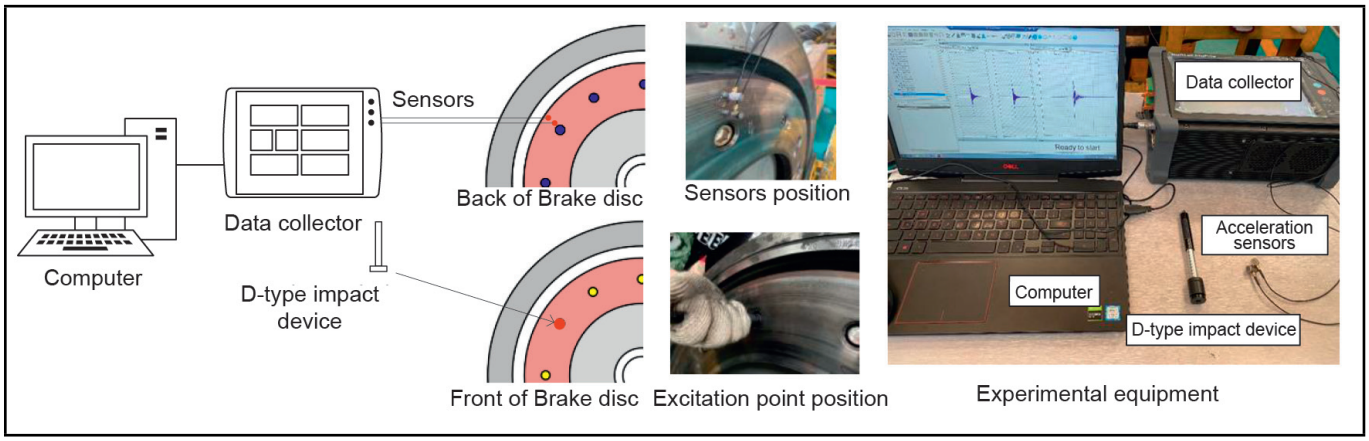

Figure 5. Experimental system.

Table 1. Detailed experimental scheme of single-bolt looseness.

Case	Torque (N·m)
1	0
2	10
3	20
4	30
5	40
6	140
7	160

amplitude of the secondary shock was higher. The separation zone between the contact interfaces can attribute to the secondary shock phenomenon. As the torque increased, the tightened bolt was aggravated and the peak amplitude of the secondary shock decreased, which means that the separation zone decreases. Figure 6(ii)(a) show the time domain signal of bolt looseness under 20 Nm torque. Compared with the completely loosened bolt signal in Fig. 6(i)(a), the peak amplitude of the secondary peak of bolt looseness under 20 Nm torque was weakened. The amplitude of the secondary shock was almost negligible when the bolt was completely tightened, as shown in Fig. 6(iii)(a). From the perspective in frequency domain, for bolt in complete loosen state, as shown in Fig. 6(i)(b), the separation zone was large and the signal coupling was strong, which resulted in severe side band modulation in the high frequency region. As the torque increased, the side bands of signal of bolt decrease in the high-frequency range, which is shown in Fig. 6(ii)(b). For bolt in completely tighten state, as shown in Fig. 6(iii)(b), the side band modulation is negligible. The vibration responses generated for different degrees of bolt looseness was variable. However, the time-frequency analysis was not sufficient to quantitively determine the looseness pattern of bolt. The original signal was nonlinear and strongly coupled under the influence of transmission path from head of bolt in front of brake disc through the disc and wheel to sensors at the back of brake disc.

The signals collected by the two different sensors were further fused through autocorrelation summation to eliminate the effect of transmission path. The fused signals were normalized to the range of -1 to 1 to avoid the influence of data distribution. The time-domain signal and frequency spectrum of the fused signal were shown in Fig. 7. The time-domain wave of the fused signal for bolt completely loosened is shown in Fig. 7(i)(a). The peak amplitude of the second shock generated due to the bolt looseness was obvious. The fused signal in Fig. 7(ii)(a) shows the same phenomena. However, the second shock was negligible in the fused signal for bolt in fully tightened state, as shown in Fig. 7(iii)(a). This means that the fused signal obtained by autocorrelation summation eliminates the influence of the transmission path and clearly expressed the shocks associated with bolt loosenes. Figure 7(b) shows the frequency spectrum of the fused signal. In the high-frequency band, the sidebands of the fusion signal became less and the main frequency was more pronounced, which means that the fused signal was less coupled than the original signal. The autocorrelation summation algorithm eliminates the influence of transmission path.

3.3. Analysis of Relative Difference of WPD Energy

Through the above analysis, the original signal of bolt under different torques in the high frequency domain shows obvious difference. The fused signals obtained by autocorrelation summation fusion of the original signals were further decomposed by 10 layers of wavelet packet decomposition (WPD) to obtain the low frequency sub signals and high frequency sub signals. The WPD energy of sub signals were further extracted to represent the feature of signal in low frequency and high frequency, as shown in Fig. 8(a) for the first 20 nodes. The WPD energy of bolt under different torques are different. The WPD energy values of the sub signal for 0 Nm and 10 Nm were similar in the first node, which also occurred in the fourth and seventh node. To enhance the difference of WPD energy under different torques, the relative difference of WPD energy e_a were calculated according to Eq. (5), as shown in Fig. 8(b). The relative difference of WPD energy e_a for different torques can be clearly distinguished at different nodes, which is beneficial to recognize the different degrees of bolt looseness.

3.4. Analysis of 1D CNN Model

The 1D CNN model was used to classify bolt looseness states. The samples to the model were energy relative difference of bolts under different torques. There were 120 samples for each torque, which were divided into 100 training samples

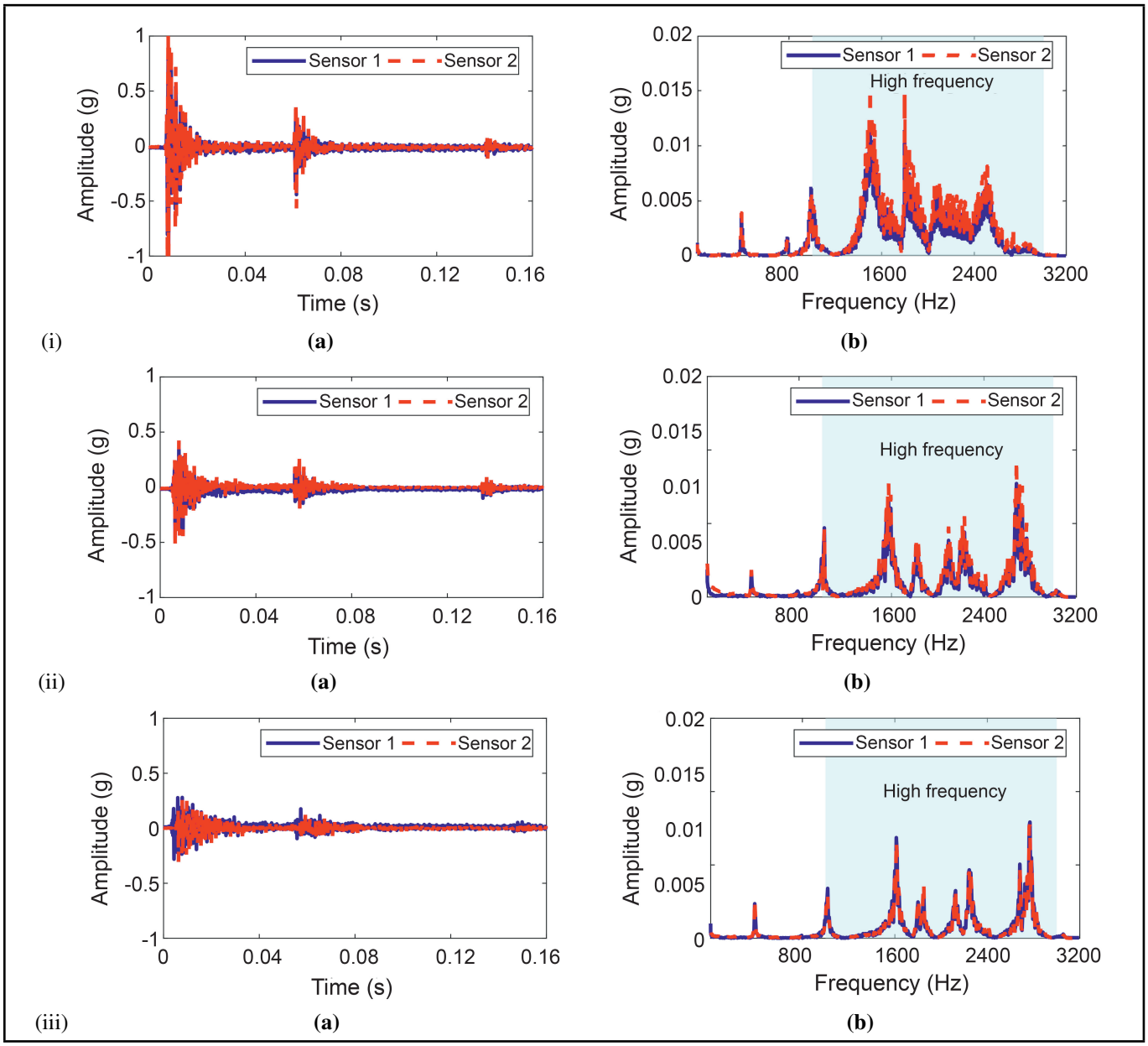

Figure 6. Example of the (a) time-domain signal and (b) frequency spectrum of #1 bolt with different torques (i) 0 N·m (ii) 20 N·m (iii) 160 N·m.

and 20 testing samples. The parameters of 1D CNN were obtained through many experiments, as shown in Table 2. The parameters of convolution layer and pool layer in a CNN was designed according to reference.[32,33] The other parameters used in calculation were iteration $N = 500$, batch size $B = 16$, learning rate $\eta = 0.001$, dropout rate $p = 0.4$.

The sample data based on energy relative difference are input into 1D CNN to train and test. The loss and accuracy curves of the proposed method are shown in Fig. 9. The loss curves of the training set and testing set almost overlapped and showed a convergence trend with small fluctuations, and the model does not fall into overfitting and underfitting. The accuracy curves of the training set and testing set both converged at around the accuracy 98.57%. The 1D-CNN model worked well. The confusion matrix of WPD-1D CNN model is shown in Fig. 10. The testing set of bolt looseness under 0 Nm, 10 Nm, 20 Nm, 140 Nm and 160 Nm torques were identified accurately. The misclassification of bolts looseness can be seen that two samples of bolt looseness under 30 Nm was misjudged the looseness degree of 40 Nm and 140 Nm. The proposed method was effective in bolt loosening detection of brake disc.

3.5. Model Comparison and Analysis

A lambda wave signal of different degree of bolt looseness are collected to combine the 1D CNN model to identify the bolt looseness.[30] Based on this, the vibration signals combined with 1D CNN is used as a comparison model. To verify the advantages of the proposed method for blot looseness detection, three different models were compared and anayzed, which include the original signal from sensor1 combined with 1D CNN model (Sensor1-1D CNN), the fused signal obtained by autocorrelation summation combined with 1D CNN model (Fused signal-1D CNN) and the proposed method.

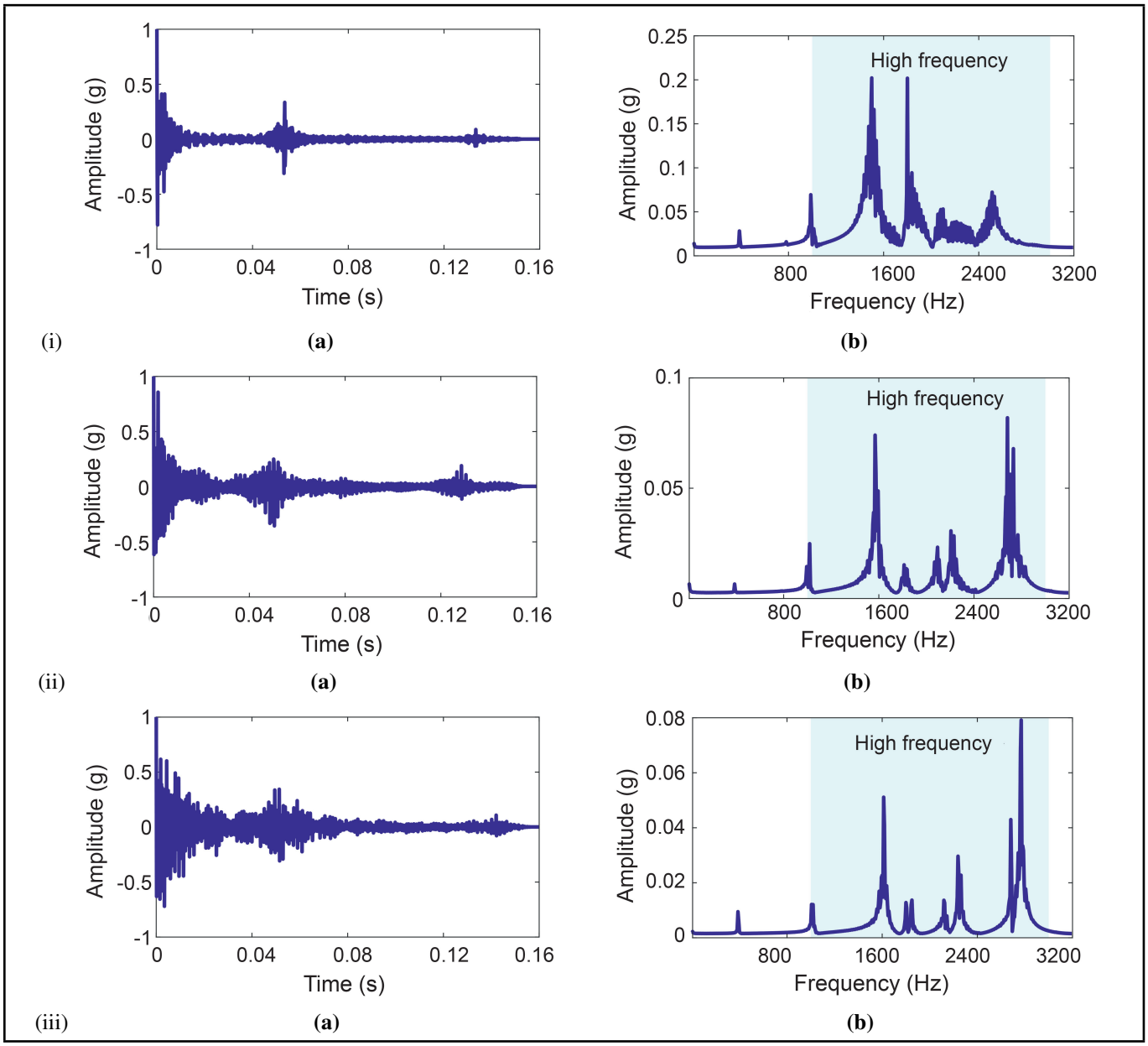

Figure 7. Example of the (a) time-domain and (b) frequency spectrum of fused signal for #1 bolt with different torques (i) 0 N·m (ii) 20 N·m (iii) 160 N·m.

The loss and accuracy were used as the indicator to evaluate the accuracy of the 1D CNN model. The original signal collected from sensor 1 was applied as the input of 1D CNN. The loss and accuracy curves of Sensor 1-1D CNN model are shown in Fig. 11(i). The loss curves of the training set and testing set almost overlapped and showed a convergence trend. Although the loss curve converges, the loss value fluctuates significantly, and the error between the predicted value and the real value of the Sensor 1-1D CNN model was large at training iterations. The accuracy curves of training set and testing set also fluctuated widely and eventually converged at around 65%. The confusion matrix of Sensor1-1D CNN model was as shown in Fig. 12(a). When the original data was used for classification, the bolts under complete looseness (0 Nm) and tightened states (140 Nm and 160 Nm) were completely identified. However, the other torques show severe misclassification of bolt looseness.

The fused signal of bolt calculated by autocorrelation summation were applied as the input of 1D CNN. The loss and accuracy curves of Fused signal-1D CNN model for bolt looseness detection are shown in Fig. 11(ii). The loss curves of the training set and testing set almost overlap and show a convergence trend, which means the training process of model was steady. There are small fluctuations in loss values. The accuracy curves of training set and testing set also fluctuate widely and eventually converge at around 92.14%. The confusion matrix of Fused signal-1D CNN model is shown in Fig. 12(b). Misclassification of bolts in different states of loosening can be seen. Most of the bolt looseness under different torques are identified accurately, and only the torque 20 Nm and 140 Nm exhibit few misclassifications.

The original signal was directly input into the 1D CNN model to train. Due to the large influence of the transmission path, the result is not satisfactory with only 70% accuracy.

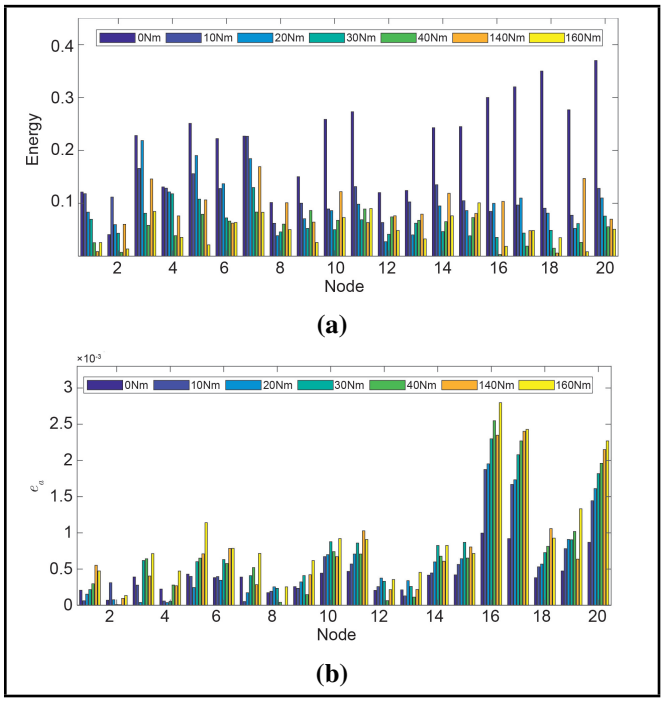

Figure 8. (a) WPD energy and (b) relative difference e_a of fused signal of bolt under different torques.

Table 2. Parameters of 1D CNN.

Layers	Size	Stride	Output	Activation Function
Input	1×1024	–	–	–
Convolution layer 1	$32 \times 1 \times 3$	1×2	$32 \times 1 \times 511$	ReLU
Convolution layer 2	$32 \times 1 \times 3$	1×2	$32 \times 1 \times 255$	ReLU
Pooling layer 1	1×2	1×2	$32 \times 1 \times 127$	Maxpooling
Convolution layer 3	$16 \times 1 \times 2$	1×2	$16 \times 1 \times 31$	ReLU
Convolution layer 4	$16 \times 1 \times 2$	1×2	$16 \times 1 \times 15$	ReLU
Pooling layer 2	1×2	1×2	$16 \times 1 \times 15$	Maxpooling
Flatten	240	–	–	–
Fully connection layer 1	120	–	–	ReLU
Fully connection layer 2	50	–	–	ReLU
Output	7	–	–	Softmax

The fused signal processed by the autocorrelation summation was input into the 1D CNN model, the accuracy was 90%, which means the influence of transmission path was eliminated. Comparing the sensor 1-1D CNN model and sate signal-1D CNN model, the proposed method combined the advantage of autocorrelation summation that can fuse the signal to effectively eliminate the influence of the transmission path and to improve the accuracy of model in quantitively identification of bot looseness. The proposed method enhanced the difference between the loosening bolt and tightening bolt by using WPD

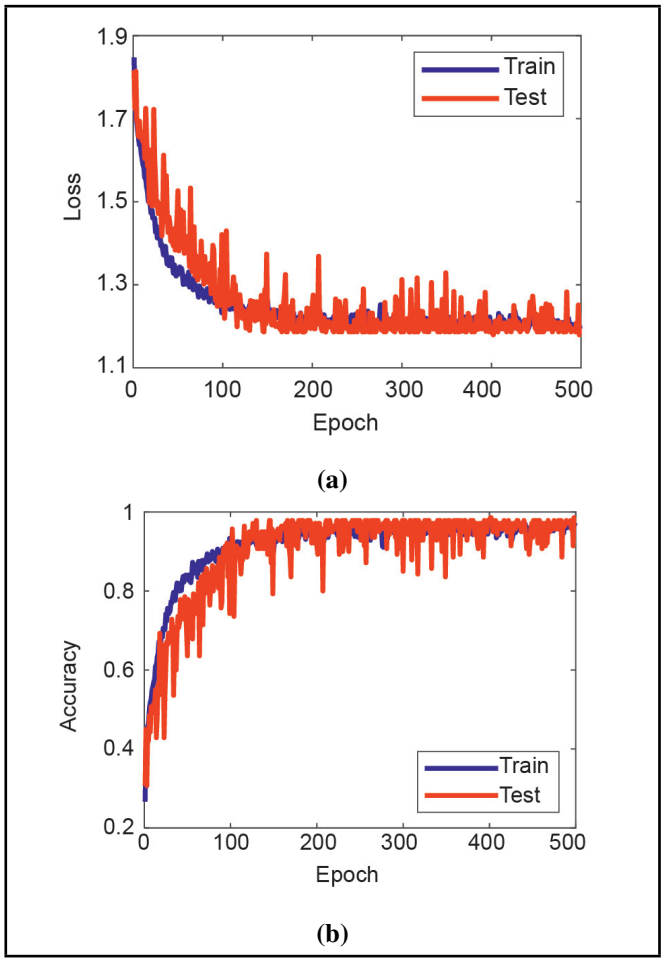

Figure 9. (a) Loss and (b) Accuracy of the WPD-1D CNN.

and the feature of relative difference of energy can further improve the recognition accuracy.

The generalization ability of the above model was verified using a 5-fold cross validation, and the results are shown in Fig. 13. The mean accuracy values of the three models including the proposed method, Sate signal-1D CNN and Sensor1-1D CNN in detecting bolt looseness are $96.7 \pm 0.6\%$, $91.3 \pm 0.7\%$, $69.6 \pm 6.3\%$, respectively. The proposed WPD-1D CNN model is more effective in detecting bolt loosening.

4. CONCLUSIONS

A method based on WPD-1D CNN is proposed to detect the bolt looseness in brake disc of high-speed rail. The proposed method solves the problem that the bolt looseness detection in brake disc of high-speed railway is influenced by the transmission path due to the complex structures of brake disc. Meanwhile, the shortcomings that both wavelet packet decomposition methods and wavelet packet energy indicators are difficult to quantitatively diagnose the bolt looseness are avoided in the proposed method. Comparing with single channel 1D CNN and fused signal CNN, the proposed method effectively takes advantage of the vibration characteristics of bolt looseness and the efficient identification capability of 1D CNN, with an accuracy rate of 97%. The most obvious changes in the brake disk after bolt looseness are structural vibration, temperature,

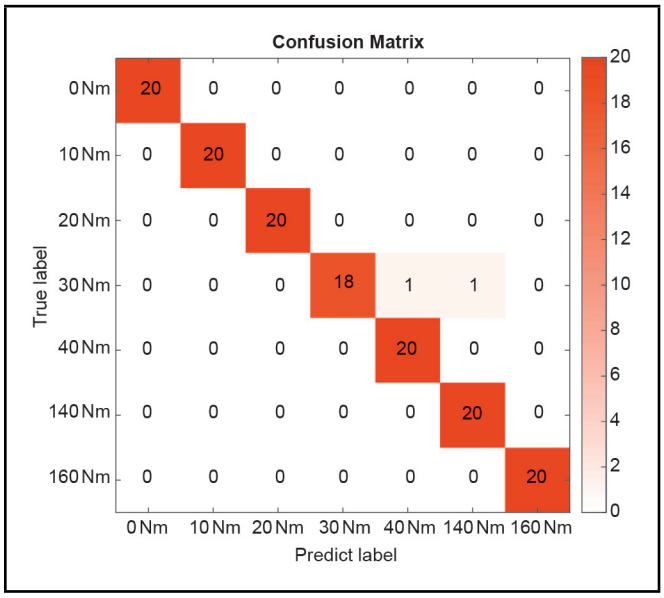

Figure 10. Confusion matrix of the WPD-1D CNN for bolt looseness detection.

and noise, etc. In the future, a method based on multimodal learning for bolt looseness detection should be studied by fusing the multi-sensors including sound signals, vibration signals and temperature signals.

ACKNOWLEDGEMENT

This work was supported by the National Natural Science Foundation of China [grant number 52275081, 51775037],, the Fundamental Research Funds for the Central Universities [grant number QNXM20220031], and Open Project Foundation of the State Key Laboratory of Traction Power in Southwest Jiaotong University [grant number TPL2307].

REFERENCES

[1] Fan, T., Ren, Z., and Xue, R. Load variation of the wheel-mounted brake disc bolts of a high-speed train, *Engineering Failure Analysis*, **119**, 105001, (2021). https://doi.org/10.1016/j.engfailanal.2020.105001

[2] Qu, J., Wang, W., Wang, B., Li, G., and Jiao, B. Analysis of the axial load of bolts of wheel-mounted brake discs of high-speed trains, *Engineering Failure Analysis*, **137**, 106250, (2022). https://doi.org/10.1016/j.engfailanal.2022.106250

[3] Nazarko, P. and Ziemianski, L. Force identification in bolts of flange connections for structural health monitoring and failure prevention, *Procedia Structural Integrity*, **5**, 460–467, (2017). https://doi.org/10.1016/j.prostr.2017.07.142

[4] Chelimilla, N., Chinthapenta, V., Kali, N., and Korla, S. Review on recent advances in structural health monitoring paradigm for looseness detection in bolted assemblies, *Structural Health Monitoring*, **22**(6), 4264–4304, (2023). https://doi.org/10.1177/14759217231158540

[5] Kong, Q., Zhu, J., Ho, S. C. M., and Song, G. Tapping and listening: a new approach to bolt looseness monitoring, *Smart Materials and Structures*, **27**, 07LT02, (2018). https://doi.org/10.1088/1361-665X/aac962

[6] Wang, F., Ho, S. C. M., and Song, G. Modeling and analysis of an impact-acoustic method for bolt looseness identification, *Mechanical Systems and Signal Processing*, **133**, 106249, (2019). https://doi.org/10.1016/j.ymssp.2019.106249

[7] Tong, F., Xu, X., Luk, B., and Liu, L. K. P. Evaluation of tile-wall bonding integrity based on impact acoustics and support vector machine, *Sensors and Actuators A: Physical*, **144**(1), 97–104, (2008). https://doi.org/10.1016/j.sna.2008.01.020

[8] Yuan, R., Lv, Y., Kong, Q., and Song, G. Percussion-based bolt looseness monitoring using intrinsic multiscale entropy analysis and BP neural network, *Smart Materials and Structures*, **28**, 125001, (2019). https://doi.org/10.1088/1361-665X/ab3b39

[9] Wang, F. and Song, G. Bolt-looseness detection by a new percussion-based method using multifractral analysis and gradient boosting decision tree, *Structural Health Monitoring*, **19**, 2023–2032, (2020). https://doi.org/10.1177/1475921720912780

[10] Wang, F., Chen, Z., and Song, G. Smart crawfish: A concept of underwater multi-bolt looseness identification using entropy-enhanced active sensing and ensemble learning, *Mechanical Systems and Signal Processing*, **149**, 107186, (2021). https://doi.org/10.1016/j.ymssp.2020.107186

[11] Jiang, J., Chen, Y., Dai, J., and Liang, Y. Multi-bolt looseness state monitoring using the recursive analytic based active technique, *Measurement*, **191**, 110779, (2022). https://doi.org/10.1016/j.measurement.2022.110779

[12] Li, N., Wang, F., and Song, G. Monitoring of bolt looseness using piezoelectric transducers: Three-dimensional numerical modeling with experimental verification, *Journal of Intelligent Material Systems and Structures*, **31**(6), 911–918, (2020). https://doi.org/10.1177/1045389X20906003

[13] Hei, C., Luo, M., Gong, P., and Song, G. Quantitative evaluation of bolt connection using a single piezoceramic transducer and ultrasonic coda wave energy with the consideration of the piezoceramic aging effect, *Smart Materials and Structures*, **29**, 027001, (2020). https://doi.org/10.1088/1361-665X/ab6076

[14] Wang, F., Chen, Z., and Song, G. Monitoring of multi-bolt connection looseness using entropy-based active sensing and genetic algorithm-based least square support vector machine, *Mechanical Systems and Signal Processing*, **136**, 106507, (2020). https://doi.org/10.1016/j.ymssp.2019.106507

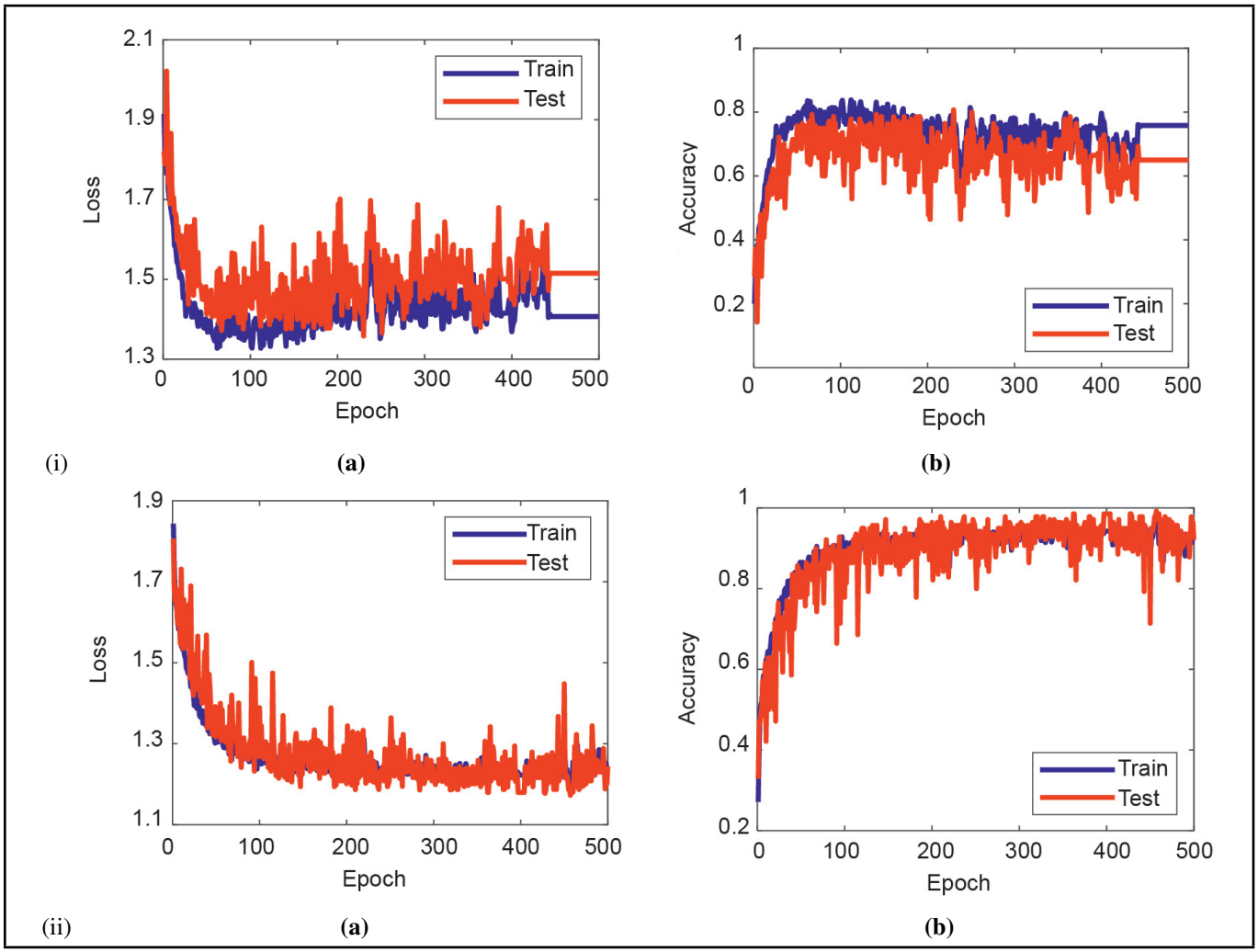

Figure 11. (a) Loss and (b) Accuracy of different model for bolt looseness detection (i) Sensor1-1D CNN (ii) Fused signal-1D CNN.

[15] Sun, W., Guan, Z., Zeng, Y., Pan, J., and Gao, Z. Bolt loosening detection of rocket connection structure based on variational modal decomposition and support vector machines, *Applied Science*, **12**, 6266, (2022). https://doi.org/10.3390/app12126266

[16] Champati, A., Voggu, S., and Lute, V. Detection of damage in bolted steel structures using vibration signature analysis, *Journal of Vibration Engineering & Technologies*, (2023). https://doi.org/10.1007/s42417-023-00916-6

[17] Zhang, X., Yan, Q., Yang, J., Zhao, J., and Shen, Y. An assembly tightness detection method for bolt-jointed rotor with wavelet energy entropy, *Measurement*, **136**, 212–224, (2019). https://doi.org/10.1016/j.measurement.2018.12.056

[18] Wang, F. and Song, G. A novel percussion-based method for multi-bolt looseness detection using one-dimensional memory augmented convolutional long short-term memory networks, *Mechanical Systems and Signal Processing*, **161**, 107955, (2021). https://doi.org/10.1016/j.ymssp.2021.107955

[19] Huynh T. C. Vision-based autonomous bolt-looseness detection method for splice connections: Design, lab-scale evaluation, and field application, *Automation in Construction*, **124**, 103591, (2021). https://doi.org/10.1016/j.autcon.2021.103591

[20] Pan, X. and Yang, T. 3D vison-based bolt loosening assessment using photogrammetry, deep neural networks, and 3D point-cloud processing, *Journal of Building Engineering*, **70**, 106326, (2023). https://doi.org/10.1016/j.jobe.2023.106326

[21] Luo, P., Wang, B., Wang, H., Ma, F., Ma, H., and Wang, L. An ultrasmall bolt defect detection method for transmission line inspection, *IEEE Transactions on Instrumentation and Measurement*, **72**, 5006512, (2023).

[22] Roy, S. S., Dey, S., and Chatterjee, S. Autocorrelation aided random forest classifier-based bearing fault detection framework, *IEEE Sensors Journal*, **20**, 10792–10800, (2020). https://doi.org/10.1109/JSEN.2020.2995109

[23] Nikula, R. P., Karioja, K., Pylvanainen, M., and Leiviska, K. Automation of low-speed bearing fault diagnosis based autocorrelation of time domain features, *Mechanical Systems and Signal Processing*, **138**, 106572, (2020). https://doi.org/10.1016/j.ymssp.2019.106572

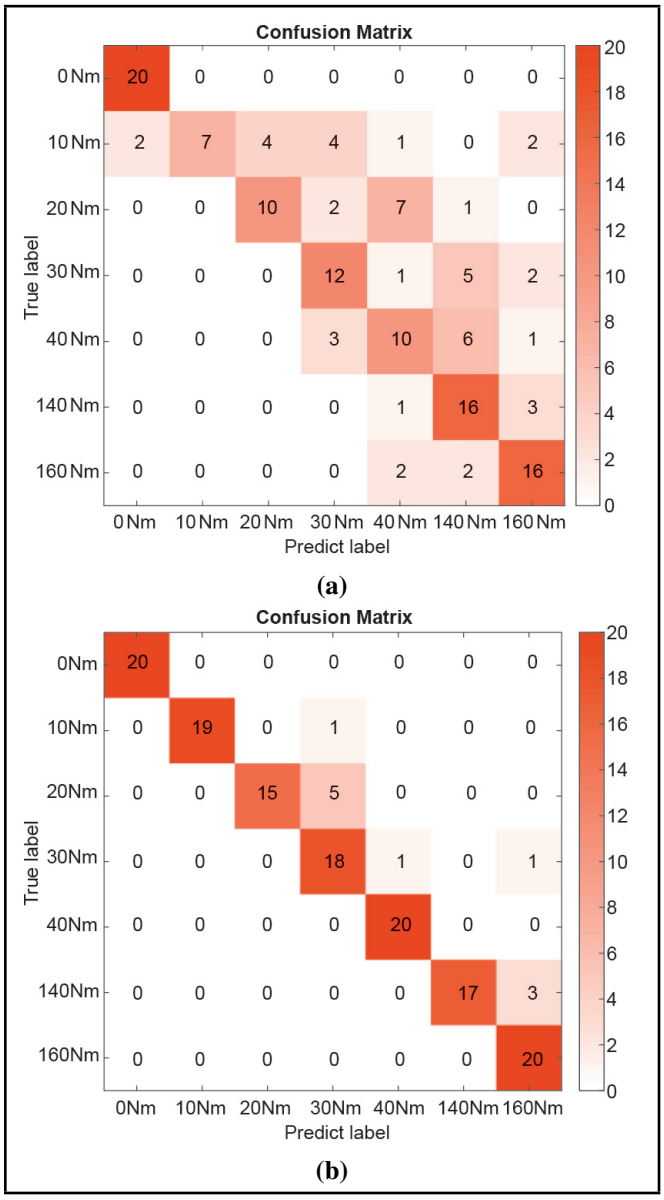

Figure 12. Confusion matrix of different model (a) Sensor1-1D CNN (b) Fused signal-1D CNN for bolt looseness detection.

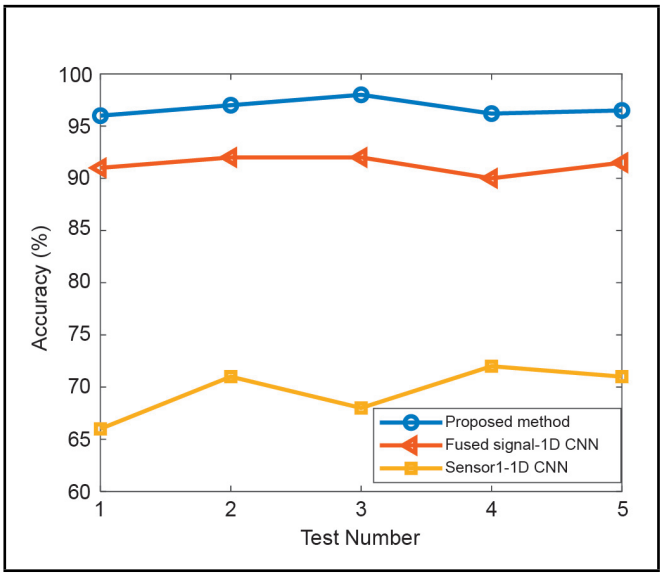

Figure 13. Results of the 5-fold cross validation.

[24] Wu, Y., Liu, L., and Qian, S. A small sample bearing fault diagnosis method based on variational mode decomposition, autocorrelation function, and convolutional neural network, *International Journal of Advanced Manufacturing Technology*, **124**, 3887–3898, (2023). https://doi.org/10.1007/s00170-021-08126-8

[25] Meyer, J. J. and Adams, D. E. Using impact modulation to quantify nonlinearities associated with bolt loosening with applications to satellite structures, Mechanical Systems and Signal Processing, **116**, 787-795, (2019). https://doi.org/10.1016/j.ymssp.2018.06.042

[26] Jiang, J., Zhang, R., Wu, Y., Chang, Ch., and Jiang, Y. A fault diagnosis method for electric vehicle power lithium battery based on wavelet packet decomposition, *Journal of Energy Storage*, **56**, 105909, (2022). https://doi.org/10.1016/j.est.2022.105909

[27] Kuai, Z. and Huang, G. Fault diagnosis of diesel engine value clearance based on wavelet packet decomposition and neural networks, *Electronics*, **12**, 353, (2023). https://doi.org/10.3390/electronics12020353

[28] Cao, Y., Sun, Y., Xie, G., and Wen, T. Fault Diagnosis of Train Plug Door Based on a Hybrid Criterion for IMFs Selection and Fractional Wavelet Package Energy Entropy, *IEEE Transactions on Vehicular Technology*, **68**(8), 7544–7551, (2019). https://doi.org/10.1109/TVT.2019.2925903

[29] Safara, F., Daraisamy, S., Azman, A., Jantan, A., Ramaiah, A. R. A. Multi-level basis selection of wavelet packet decomposition tree for heart sound classification, *Computers in Biology and Medicine*, **43**(10), 1407–1414, (2013). https://doi.org/10.1016/j.compbiomed.2013.06.016

[30] Pandey, P., Rai, A., and Mitra, M. Explainable 1-D convolutional neural network for damage detection using Lamb wave, *Mechanical Systems and Signal Processing*, **164**, 108220, (2022). https://doi.org/10.1016/j.ymssp.2021.108220

[31] Chen, Z., Cryllias, K., and Li, W. Mechanical fault diagnosis using convolutional neural networks and extreme learning machine, Mechanical Systems and Signal Processing, **133**, 106272, (2019). https://doi.org/10.1016/j.ymssp.2019.106272

[32] Guo, Y., Zhou, Y., Zhang, Z. Fault diagnosis of multichannel data by the CNN with the multilinear principal component analysis, *Measurement*, **171**, 108513, (2021). https://doi.org/10.1016/j.measurement.2020.108513

[33] Zhang, W., Li, C., Peng, G., Chen, Y., and Zhang, Z. A deep convolutional neural network with new training methods for bearing fault diagnosis under noisy environment and different working load, *Mechanical Systems and Signal Processing*, **100**, 439–53, (2018). https://doi.org/10.1016/j.ymssp.2017.06.022